Influence of Crystalline Forms of Titania on Desorption/Ionization Efficiency in Titania-Based Surface-Assisted Laser Desorption/Ionization Mass Spectrometry

Hideya KAWASAKI, Kouji OKUMURA, and Ryuichi ARAKAWA*

Department of Chemistry and Materials Engineering, Faculty of Chemistry, Materials and Bioengineering, Kansai University, Suita, OSAKA, JAPAN

In surface-assisted laser desorption/ionization mass spectrometry using titania (TiO_2) films (TiO_2-SALDI-MS), one of the most important aspects is the absence of matrix interferences in the low-mass region. Therefore, in TiO_2-SALDI, the detectable mass range for small biomolecules, pharmaceutical compounds, amino acids, and oligopeptides can be extended to below *m/z* 500. The physicochemical properties of titania are dependent on the crystalline form of the material; however, thus far, very little attention has been given to the effect of the crystalline form of titania on titania-based SALDI-MS. We investigated the influence of crystalline forms on the desorption/ionization efficiency of TiO_2-based SALDI-MS using different crystalline forms such as rutile, anatase, and a non-crystalline amorphous structure. On the basis of survival yield measurements using benzylpyridium chloride, and the desorption/ionization efficiency of peptides (angiotensin II and gly-gly-tyr-arg) and saccharides (cellobiose and hexa-*N*-acetyl-chitohexaose), it was found that the anatase-type TiO_2 is suitable for the TiO_2-based SALDI-MS. Rutile-type TiO_2 lost the SALDI activity compared with TiO_2 in other crystalline forms, although rutile-type TiO_2 showed the highest UV absorbance.

(Received June 14, 2010; Accepted September 21, 2010)

1. Introduction

Matrix-assisted laser desorption/ionization mass spectrometry (MALDI-MS) using organic matrices is a soft ionization technique that causes significantly less fragmentation of the analytes.[1), 2)] By using UV-absorbing organic acids such as 2,5-dihydroxybenzoic acid (DHBA) and α-cyano-4-hydroxycinnamic acid (CHCA) in MALDI-MS, it is possible to analyze various compounds such as polymers, peptides, and lipids, as well as complex mixtures in high-salt matrices and buffers.[3), 4)] However, the matrix ion interface and detector saturation are inevitable consequences in the MALDI-MS analysis of low-mass molecules ($<m/z$ 500), and this makes the characterization of small molecules difficult despite the significance of such characterization. Various approaches involving the use of organic-matrix-free LDI-MS have been investigated for analyzing small molecules using a MALDI instrument.[5)] Siuzdak and co-workers developed a matrix-free LDI-MS method for generating intact molecular ions by using porous silicon, which has a high UV absorbance and a high surface area.[6)] This method is known as desorption ionization from porous silicon (DIOS). In contrast to MALDI, DIOS does not involve the use of organic matrices, and hence, one of the most important features of DIOS is the absence of matrix interference in the low-mass region. Therefore, in DIOS, the detectable mass range for small biomolecules, such as pharmaceutical compounds, amino acids, and oligopeptides can be extended to below *m/z* 500.[7)–9)]

Since then, several other types of nanostructured substrates for organic-matrix-free LDI-MS have been reported. In particular, silicon-based nanomaterials, including nanostructured silicon films,[10)] silicon nanowires,[11), 12)] silicon nanocavity arrays,[13), 14)] silicon microcolumn arrays,[15)] and amorphous silicon[16)] have been studied extensively, and a new technique known as nanostructure-initiator mass spectrometry (NIMS) has been recently proposed.[17)] Metal-oxide-based semiconductors with good UV absorbance are also promising candidates for matrix-free LDI-MS applications, such as titania sol-gel films,[18)] titania nanotube arrays,[19)] zinc oxide nanowires,[20)] mesoporous tungsten titanium oxides,[21)] and germanium nanodots.[22)] In addition, double- or multilayer-coated hybrid substrates such as metal-coated porous alumina (platinum/alumina),[23), 24)] two-layered amorphous silicon,[25)] titania-printed aluminum foils (titania/aluminum),[26)] silver-particle-deposited porous silicon (silver/silicon),[27)] gold nanorods on porous alumina (gold/alumina),[28)] layer-by-layer (LBL) self-assembled films (polymer/gold),[29)] Pt nanoflowers on a scratched silicon,[30)] DVDs coated with diamond-like carbon,[31)] and cationic-polymer-coated graphite sheets (polymer/graphite)[32)] are considered to be promising materials for matrix-free LDI-MS because the layer properties of these substances can be varied independently. Further, these hybridization effects can improve the efficiency of matrix-free LDI-MS. In this paper, "surface-assisted laser desorption/ionization" (SALDI) refers to the

* Correspondence to: Ryuichi ARAKAWA, *Department of Chemistry and Materials Engineering, Faculty of Chemistry, Materials and Bioengineering, Kansai University, 3–3–35 Yamate-cho, Suita-shi, Osaka 564–8680, JAPAN*, e-mail: arak@kansai-u.ac.jp

nanostructured substrates, although the meaning of the technical terms used in this field is slightly unclear.

Among the various types of materials proposed for SALDI-MS, titania (TiO_2) appears to be a promising candidate, because its physicochemical properties permit SALDI performance to be improved: (1) a high UV absorbance with a large bandgap (bulk anatase: 3.2 eV), (2) good chemical stability under a variety of pH conditions and under ambient air, (3) surface modification with various functional groups,[33] and (4) possible morphology control of titania such as porous structures with a high surface area.[18), 19)] In addition, in contrast to DIOS-MS that is used for analyzing analytes with a molecular weight of <6 kDa,[34] titania-based SALDI-MS can be used to analyze high molecular weight proteins (<24 kDa) as well as small molecules and has the advantage that phosphopeptides are specifically adsorbed.[18), 19), 35)] The physicochemical properties of titania depend on the crystalline form.[36] Therefore, in order to further develop titania-based SALDI-MS, investigating the influence of crystalline form on the desorption/ionization efficiency of titania-based SALDI-MS becomes an important issue, since it would provide useful information on the fundamental parameters that determine the desorption/ionization process. However, thus far, very little attention has been given to the effect of the crystalline form of titania on titania-based SALDI-MS.

The purpose of this study was to investigate the influence of crystalline form on the desorption/ionization efficiency of titania-based SALDI-MS. It is known that titania can exist in one of the following three bulk crystalline forms: rutile, anatase, or brookite. In this study, we used two crystalline forms of titania, rutile and anatase, along with a non-crystalline amorphous structure. Here, we used a titania thin film without porous structures as the SALDI substrate. We employed benzylpyridium chloride (BP-Cl) as the "hermometer ion" to examine the desorption efficiency of titania-based SALDI-MS as a measure of the extent of internal energy transfer in the desorption process based on survival yield measurements.[30] We also compared the survival yield values of BP-Cl among titania-based SALDI-MS, DIOS-MS, and MALDI-MS with CHCA. Finally, the desorption/ionization efficiency of peptides (angiotensin II and gly-gly-tyr-arg) and some saccharides (cellobiose and hexa-*N*-acetyl-chitohexaose) was examined in titania-based SALDI-MS using the above three crystalline forms of titania.

2. Experimental

2.1 Materials and reagents

Acetone, methanol, ethanol, insulin and trifluoroacetic acid (TFA), D(+)-cellobiose, triammonium citrate, citric acid and H_3PO_4 were purchased from Wako Pure Chemicals (Osaka, Japan). Hexa-*N*-acetylchitohexaose was purchased from Seikagaku Corp. (Tokyo, Japan). The oligopeptide, gly-gly-tyr-arg (GGYR) was purchased from Peptide Institute, Inc. (Osaka, Japan). α-Cyano-4-hydroxycinnamic acid (CHCA), benzyl chloride, and anhydrous pyridine were purchased from Sigma Aldrich (St. Louis, MO). All of these reagents were used as received and were used without further purification. Silicon wafers ($\langle 100 \rangle$, n-type, 0.012–0.02 Ω-cm) were purchased from Sumco Co. (Tokyo, Japan). Titanium sheets (thickness: 0.1 mm, purity: 99.5%) were purchased from Nilaco Co. (Tokyo, Japan).

2.2 Preparation of titania films

A titanium foil (thickness: 0.1 mm, purity: 99.5%) was cut into 1.5 cm × 1.5 cm squares, cleaned with methanol in an ultrasonic bath, rinsed with deionized water, and finally dried in air. The electrolyte was a 1.4 M aqueous H_3PO_4 solution. An amorphous titania film was prepared by potentiostatic anodization (7651, Yokogawa Co., Japan) at a constant voltage of 70 V for 1 min at room temperature using a Pt cathode.[37] A schematic representation of the equipment used for preparing the titania film is shown in Fig. 1. The thickness of the thin titania films was estimated to be approximately 60 nm ± 15 nm on the basis of the interference color of the film.[38] After the electrochemical treatment, the titania substrate was rinsed with deionized water and dried in a nitrogen stream. In order to obtain an anatase-type titania film, thermal annealing was conducted at 450℃ for 3 h in ambient air using a KDF-S 70 thermoannealer (Denken Co., Japan); the annealing temperature was increased to 450℃ at a heating rate of 30℃/min.[39] A rutile-type titania film was obtained by thermal annealing at 1,000℃ for 3 h in ambient air; the annealing temperature was increased up to 1,000℃ at a heating rate of 30℃/min.[39] A scanning electron microscope (SEM, JEOL JSM-6700) was used to observe the surface morphology at an accelerating voltage of 5.0 kV. Several straight lines from the crystal grain boundary were observed for rutile-type and anatase-type titania films but not for non-crystalline amorphous titania, as

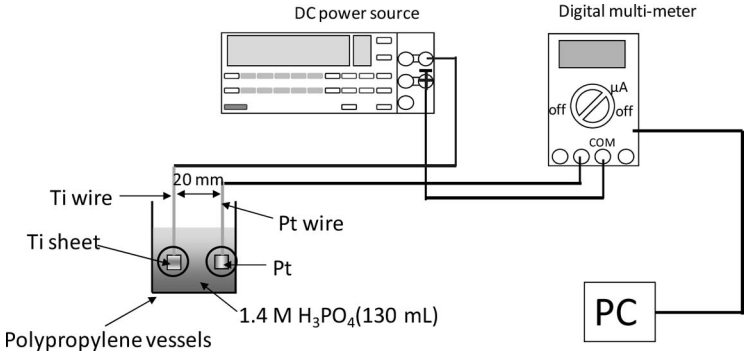

Fig. 1. Schematic representation of equipment used in preparing titania films by potentiostatic anodization.

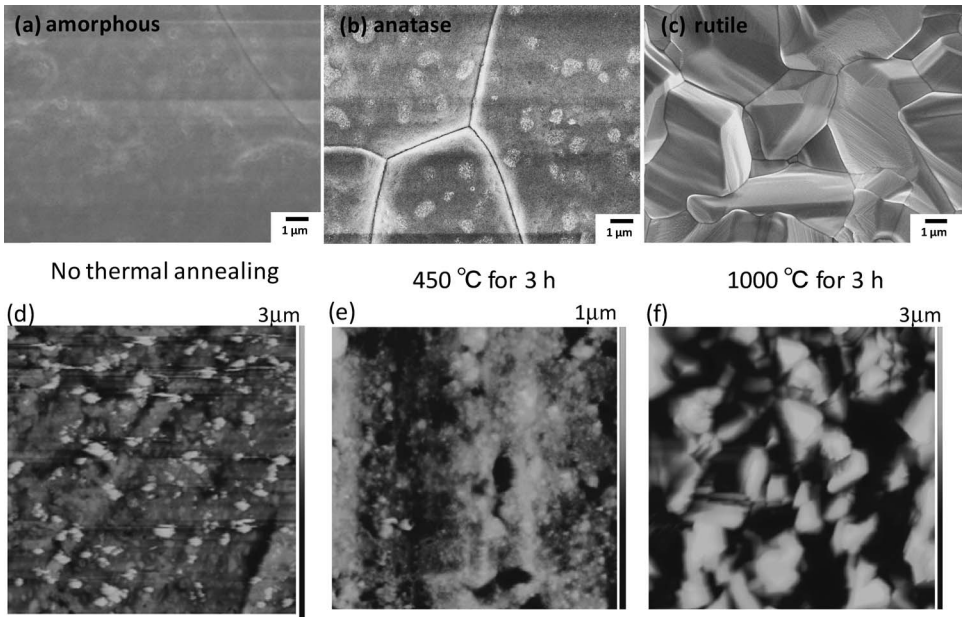

Fig. 2. SEM images of (a) amorphous titania film without no thermal annealing, (b) anatase titania film with thermal annealing at 450℃ for 3 h, and (c) rutile titania film with thermal annealing at 1,000℃ for 3 h. The corresponding AFM images (50 μm×50 μm) (d) the amorphous titania film, (e) the anatase titania film, and (f) the rutile titania film.

shown in Figs. 2a, 2b, and 2c. The AFM images were obtained, by atomic force microscopy(AFM) in tapping modes on a NanoScope IIIa (Veeco) with a scan rate of 0.5 Hz using silicon tips of a nominal spring constant of 42 $N \cdot m^{-1}$ in air. The arithmetic mean deviations (*Ra*) of the profiles of the titania films were estimated to be 180 nm for the non-crystalline amorphous titania film (Fig. 2d), 102 nm for the anatase-type titania film (Fig. 2e), and 580 nm for the rutile-type film (Fig. 2f), respectively. This indicates all of the titania films used in this study had a roughness in the sub-micron order range.

2.3 Preparation of DIOS chips

DIOS chips were prepared as described in the literature.[16] In a typical experiment, n-type silicon (100) wafers having a resistivity of 1–3 Ω-cm were anodically etched (30 mA cm^{-2}, 1 min) in a 1 : 1 (v/v) solution of EtOH–HF (46%) under exposure to white light from a 100-W tungsten filament bulb located at a distance of 30 cm. After the etching, the DIOS chips were washed with EtOH and dried in a vacuum. The formation of submicron-sized porous structures was confirmed from scanning electron microscope (SEM) images of the DIOS chips.

2.4 SALDI-MS

The substrates prepared for SALDI-MS were fixed to a stainless-steel sample plate using double-sided conductive carbon tape. The sample solution, containing 0.5 μL of a cationization agent (0.1% TFA or 1 mM NaI), was spotted on this substrate and dried under reduced pressure. SALDI mass spectra were obtained in the linear mode using an AXIMA CFR TOF mass spectrometer (Shimadzu, Kyoto, Japan) fitted with a pulsed nitrogen laser (337 nm). One hundred laser shots were used for acquiring the mass spectra. The analyte ions were accelerated at 20 kV under delayed extraction conditions.

2.5 Survival yield (SY) measurements of thermometer ions

Benzylpyridinium chloride (BP-Cl) was synthesized by the reaction of pyridine (anhydrous, purity: >99.8%, Sigma Aldrich) and the corresponding substituted benzyl chloride (purity: 95–99%, Sigma Aldrich).[40] Benzyl chloride was mixed with 3 mL of anhydrous pyridine (pyridine/benzyl halide molar ratio: 20 : 1), and this solution was then heated in a water bath for 5 h at 60℃. Excess pyridine was removed by vacuum evaporation. The compounds with BP-Cl were confirmed by a SALDI-MS analysis and were used without further purification. A stock solution of BP-Cl (0.166 mM) was prepared in methanol. For insulin, an aqueous solution of the sample was mixed with an aqueous citrate solution [triammonium citrate (50 mM)/citric acid (100 mM), 3 : 1 (v/v)] for SALDI-MS analysis.

3. Results and Discussion

3.1 Survival yield measurements of thermometer ions in titania-based SALDI-MS

In the SALDI process, excess energy may be transferred to individual molecules; this may lead to undesired fragmentation, as opposed to the soft desorption that occurs in MALDI. In order to examine the degree of internal energy transfer in the desorption process for titania-based SALDI-MS, we measured the survival yield (SY) of a model compound, benzylpyridine, which affords a series of benzylpyridinium ions, the so-called "thermometer (TM) ions." Details of the SY method using TM ions have been previously reported in the literature.[41)–44)] We performed the SY measurements of BP-Cl in SALDI-MS using titania films with different crystalline forms (rutile, anatase, and a non-crystalline amorphous structure). The SALDI mass spectrum of BP-Cl exhibits two primary

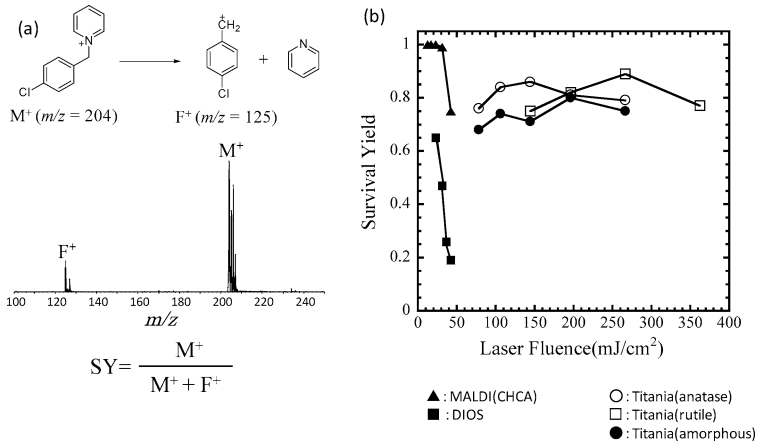

Fig. 3. (a) SALDI mass spectrum of BP-Cl using titania films with different crystalline forms (rutile, anatase, and a non-crystalline amorphous structure). Comparison of molecular ion survival yields for BP-Cl in DIOS and in MALDI with a CHCA matrix.

Table 1. Laser Threshold Values for Titania-Based SALDI-MS

	Amorphous (mJ/cm^2)	Anatase (mJ/cm^2)	Rutile (mJ/cm^2)
GGYR, $[M+H]^+$	37	43	Not detected
Angiotensin II, $[M+H]^+$	42	45	115
Cellobiose, $[M+Na]^+$	60	57	Not detected
Hexa-*N*-acetyl-chitohexasose, $[M+Na]^+$	62	49	82

peaks: a molecular ion M^+ peak (*m/z* 204) and the corresponding fragment F^+ peak (benzyl cation, *m/z* 125), as shown in Fig. 3a. The SY value can be determined using the following equation:

$$SY = I_M/(I_M + I_F) \quad (1)$$

where I_M and I_F are the experimentally measured intensities of the M^+ and F^+ peaks, respectively. The internal energy is inversely proportional to SY. The change in the SY of BP-Cl with laser fluence was also examined. For the sake of comparison, SY measurements were also carried out on DIOS and on MALDI with CHCA. Figure 3b shows the survival yield (SY) values for the titania, DIOS, and MALDI. The survival yield (SY) values using the titania film are lower than those of MALDI (*i.e.*, higher fragmentation tendency). The SY values remain practically unchanged (SY: 0.7–0.8) irrespective of the crystalline forms of titania, although the amorphous-type titania showed slightly small SY values. This indicates that the crystalline forms of titania do not have a major impact on survival yield. However, the laser threshold value for ion production for BP-Cl in the rutile-type titania (~150 mJ/cm^2) is considerably higher than that of anatase- and amorphous-type titania (~80 mJ/cm^2). This issue is discussed below.

The SY values of the titania film are larger than those of DIOS (SY: 0.7–0.2), indicating less fragmentation of BP-Cl for the titania film than in the case of DIOS. This is consistent with the previous finding that DIOS showed low SY values (SY: 0.4–0.1).[44] The difference between DIOS and the titania film can be attributed to the different dimensionality of plume expansion.[41), 42)] While for the nanopores in DIOS plume expansion is quasi-one dimensional,[42)] for a titania film without a porous structure the expansion of the desorbed plume may be three dimensional. This suggests that the confinement of the DIOS plume in the nanopores results in a more efficient energy transfer than that in the three-dimensional unobstructed expansion for the case of a titania film; hence, the SY values of DIOS decrease at a high laser fluence.[41)]

3.2 Laser threshold for titania-based SALDI-MS

The minimum laser energy required for generating stable ion signals (*i.e.*, laser threshold) is an important benchmark for characterizing the effectiveness of MALDI,[45)] SALDI,[23), 46)] and DIOS.[42), 44)] In this study, we examined the laser threshold for BP-Cl, angiotensin II, GGYR, cellobiose, and hexa-*N*-acetyl-chitohexaose in titania-based SALDI-MS. The electrical conductivity (κ) and the specific heat capacity (C_p) of titania are similar for the rutile and anatase structures (C_p = ~0.169 cal/K_g* and $\kappa = 10^{-13}$–10^{-14} ohm/cm). On the other hand, rutile-type titania has the highest UV absorbance among these crystalline forms.[39)] From the viewpoint of the thermal desorption process, a high UV absorbance for rutile-type titania would require the lowest fluence threshold. Surprisingly, we found that the rutile-type titania required the highest fluence threshold to initiate desorption (*i.e.*, low desorption efficiency at a given laser irradiation). The laser threshold value for ion production of BP-Cl in the rutile-type titania (~150 mJ/cm^2) is much higher than that of anatase- and amorphous-type titania (~80 mJ/cm^2), as shown in Fig. 3b.

A low desorption/ionization efficiency of SALDI-MS based on rutile-type titania was also observed for peptides and saccharides. Table 1 shows the laser threshold for titania-based SALDI-MS for GGYR, angiotensin II, cellobiose, and hexa-*N*-acetyl-chitohexaose. The

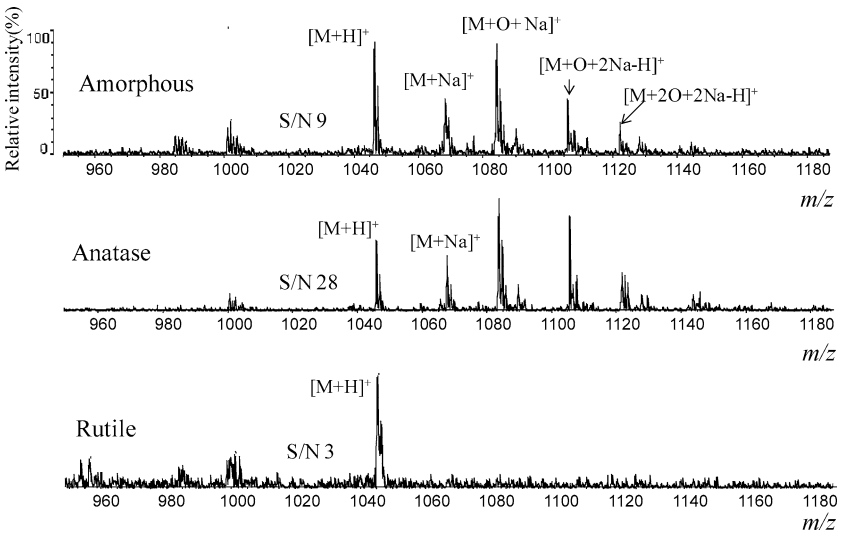

Fig. 4. Titania-based SALDI mass spectra of angiotensin II (20 pmol), using different crystalline forms (rutile, anatase, and a non-crystalline amorphous structure).

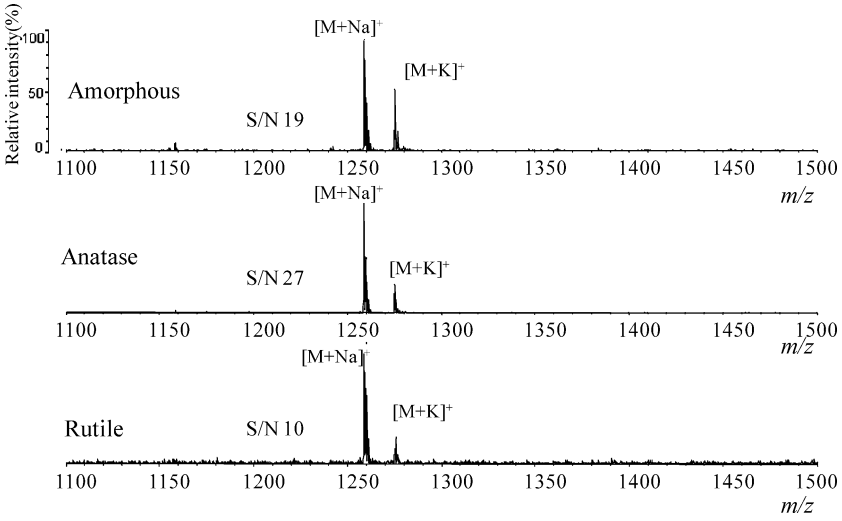

Fig. 5. Titania-based SALDI mass spectra of hexa-*N*-acetyl-chitohexaose (100 pmol), using different crystalline forms (rutile, anatase, and a non-crystalline amorphous structure).

rutile-type titania required the highest fluence threshold to initiate the desorption/ionization of angiotensin II and hexa-*N*-acetyl-chitohexaose; the corresponding mass spectra are shown in Fig. 4. The detection of peptides was difficult in the case of rutile-type titania. Rutile-type titania can be used only for detecting angiotensin II at a high laser fluence, and the signal-to-noise ratio is very low with a poor peak resolution, as shown in Fig. 4a. On the other hand, anatase-type titania has the lowest laser fluence threshold for initiating the desorption/ionization of analytes and the higher signal-to-noise ratio examined in this study, as shown in Table 1, Figs. 4 and 5. Thus, it can be concluded that anatase-type titania is the most suitable for TiO_2-based SALDI-MS. Insulin, a relatively low molecular weight protein, was detectable when anatase-type titania based SALDI-MS was used with a citrate buffer, while the detection of deprotonated ions of angiotensin II in the negative-ion mode was difficult when using the anatase-type titania form, as in the case of the DIOS chips[47] (Fig. 6).

Under the UV-laser irradiation on titania based SALDI-MS, it was reported that electrons are excited from the valence band to the conduction band of titania, producing oxidative holes to drive in-source oxidation reactions and reductive electrons to induce in-source reactions of analytes in SALDI-MS.[33), 48), 49)] In this study, such UV-laser induced photocatalytic oxidation reactions were observed in the case of amorphous (or titania)-type titania with strong photocatalytic effects, but not for rutile-type titania with weak photocatalytic effects. As shown in Fig. 4, several peaks except for protonated ion and metal adduct ions of angiotensin II were observed only when amorphous(or titania)-type titania was used, which may be responsible for the oxidation products of angiotensin II through the photocatalytic oxidation reactions. Tentative assignments for the oxidation products are shown in Fig. 4. In the case of hexa-*N*-acetyl-chitohexaose, an oxidation product was not observed (Fig. 5). It should be noted that such UV-laser induced photocatalytic oxidation products of angiotensin II cannot be detected when citrate buffer is used as the proton source, and only protonated ion of the peptide was detected.[33)] The

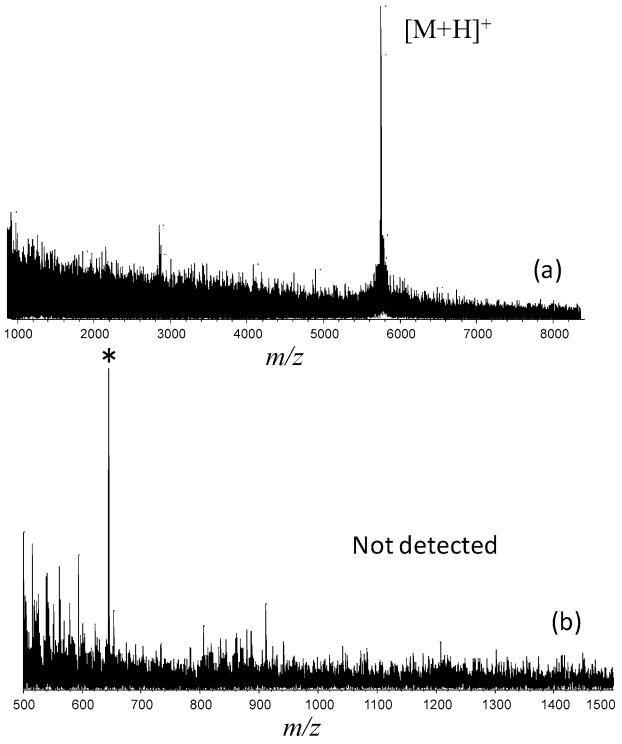

Fig. 6. Anatase type's titania-based SALDI mass spectra of (a) insulin (60 pmol) in the positive ion mode and (b) angiotensin II (20 pmol) in the negative ion mode. The peak denoted by (*) is assigned to contamination of the titania substrate.

use of citrate buffer may be useful for suppressing photocatalytic oxidation reactions of analytes in titania-based SALDI-MS.

3.3 Factors affecting the desorption/ionization efficiency of titania-based SALDI-MS

There is no consensus regarding the mechanism underlying SALDI, but the physicochemical properties required to promote the desorption/ionization efficiency may be summarized as follows: (1) laser-induced rapid temperature increase,[50] (2) substrates with a high surface area (porous, groove-like, nanowires, and nanodots),[50), 51] (3) solvent molecules,[41), 52] (4) surface functionalities such as terminal-OH groups or a hydrophobic surface,[12), 16), 42), 43), 53] (5) an electrically conductive surface,[23] and (6) laser-induced surface melting/restructuring.[40), 46), 54] Among these factors, the laser-induced rapid temperature increase of the SALDI substrate has been widely regarded as the thermal desorption of analyte molecules without thermal decomposition in organic matrix-free LDI-MS.[1] The peak temperature will be a function of the optical absorption coefficient, heat capacity, and heat conductivity of the substrate being investigated. In particular, a high optical absorption coefficient of the substrate enhances the rapid temperature increase during the SALDI process. Low thermal conductivity confines the heat near the surface in order to increase the peak temperature, thereby being effective in transferring energy from the surface to the analyte. Surface morphologies can also affect the laser-induced rapid temperature increase of a SALDI substrate. For example, the increased surface porosity of porous silicon is known to result in a decrease in the thermal conductivity of porous silicon [1.2 W (m.K)] depending on the porosity as compared to a single-crystalline silicon wafer without a porous structure [~130 W (m.K)].[14] As a result, the use of porous silicon results in a decrease in the minimum laser irradiation energy for analyte desorption, compared to the use of a titania film without a porous structure, as shown in Fig. 3b.

The rutile-type titania has a higher UV absorbance for effective SALDI than the anatase-type or the amorphous-type titania. However, the findings of this study indicate that rutile-type titania is not suitable for use in conjunction with SALDI-MS. This implies that non-thermal desorption contributes to the desorption/ionization process in SALDI based on the anatase (or amorphous)-type titania. There may be two possible contributions by non-thermal desorption in titania-based SALDI-MS: (1) the presence of surface terminal-OH groups and (2) laser-induced surface melting/restructuring. It has been reported that the surface hydroxyl groups of titania diminish with increasing temperature and almost disappear at 700℃ because the surface hydroxyl groups are removed by desorption.[55] Therefore, it is reasonable to assume that the density of hydroxyl groups in the rutile-type titania prepared at 1,000℃ in this study is very low as compared to anatase-type titania prepared at 450℃ or amorphous-type titania prepared without heating. Therefore, it is likely that the rutile-type titania lost its SALDI activity because the surface hydroxyl groups were eliminated during the thermal heating at 1,000℃. This is consistent with the findings of a previous study that amorphous silicon loses its SALDI activity upon the hydrogenation of surface hydroxyl groups.[16] By these surface physicochemical properties, a thin layer of water that is absorbed to the silicon surface via surface hydroxyl groups is thought to facilitate analyte solvation and aid the desorption of the analyte.[41), 49] Such a thin layer of water molecules absorbed to the titania surface via surface hydroxyl groups may also assist in the desorption of the analyte in anatase (or amorphous)-type titania-based SALDI-MS.

Another possible non-thermal desorption process in anatase (or amorphous)-type titania-based SALDI is laser-induced surface melting/restructuring.[40), 46), 54] Rutile crystals are the most stable among titania crystals at high temperatures. As a result, anatase crystals (or amorphous structures) may be converted into rutile crystals upon laser-induced heating. In titania-based SALDI-MS, the laser-induced surface phase transition from the anatase (or amorphous) type to the rutile type might occur, resulting in assisting the desorption of the analyte.

4. Conclusion

We investigated the influence of crystalline form on the desorption/ionization efficiency of TiO_2-based SALDI-MS using different crystalline forms: rutile, anatase, and a non-crystalline amorphous structure. The survival yield (SY) values remained practically unchanged (SY: 0.7–0.8) irrespective of the crystalline form of titania employed. This indicates that the crys-

talline form of titania does not have a major impact on survival yield (the degree of fragmentation). However, the laser threshold value for ion production for BP-Cl in rutile-type titania (~150 mJ/cm^2) was considerably higher than that of anatase- and amorphous-type titania (~80 mJ/cm^2). On the basis of the desorption/ionization efficiency of peptides (angiotensin II and gly-gly-tyr-arg) and saccharides (cellobiose and hexa-*N*-acetyl-chitohexaose), the rutile-type titania lost SALDI activity in spite of the fact that its UV absorbance is higher than that of the anatase (or amorphous)-type titania. The non-thermal desorption of surface terminal-OH groups and laser-induced surface melting/restructuring is proposed in the anatase (or amorphous)-type titania-based SALDI process.

Acknowledgments

This study was partially supported by a Grant-in-Aid for Scientific Research (B) (No. 22350040 from the Japan Society for the Promotion of Science (JSPS) and by the Core-to-Core Program promoted by the Japan Society for the Promotion of Science (Project No. 18004). This study was also supported by the "Strategic Project to Support the Formation of Research Bases at Private Universities: Matching Fund Subsidy from MEXT (Ministry of Education, Culture Sports, Science and Technology of Japan).

References

1) K. Tanaka, H. Waki, Y. Ido, S. Akita, Y. Yoshida, and T. Yoshida, *Rapid Commun. Mass Spectrom*., **2**, 151 (1988).
2) M. Karas, D. Bachmann, and F. Hillenkamp, *Anal. Chem*., **57**, 2935 (1985).
3) (a) W. F. Nielen, *Mass Spectrom. Rev*., **18**, 309 (1999). (b) S. D. Hanton, *Chem. Rev*., **101**, 527 (2001). (c) K. Deiseweard, *Chem. Rev*., **103**, 395 (2003). (d) M. Karas, R. Kruger, *Chem. Rev*., **103**, 427 (2003). (e) R. Knochenmuss, R. Zenobi, *Chem. Rev*., **103**, 441 (2003).
4) F. Hillenkamp and J. Peter-Katalinić, "MALDI-MS: A Practical Guide to Instrumentation, Methods and Applications, Small-Molecule Desorption/Ionization Mass Analysis in Chapter 9," Wiley-Vch (2007).
5) D. S. Peterson, *Mass Spectrom. Rev*., **26**, 19 (2007).
6) J. Wei, J. M. Buriak, and G. Siuzdak, *Nature*, **399**, 243 (1999).
7) R. A. Kruse, S. S. Rubakhin, E. V. Romanova, P. W. Bohn, and J. V. Sweedler, *J. Mass Spectrom*., **36**, 1317 (2001).
8) Z. Shen, J. J. Thomas, C. Averbuj, K. M. Broo, M. Engelhard, J. E. Crowell, M. G. Finn, and G. Siuzdak, *Anal. Chem*., **73**, 612 (2001).
9) E. P. Go, J. E. Prenni, J. Wei, A. Jones, S. C. Hall, H. E. Witkowska, Z. Shen, and G. Siuzdak, *Anal. Chem*., **75**, 2504 (2003).
10) J. D. Cuiffi, D. J. Hayes, S. J. Fonash, K. N. Brown, and A. D. Jones, *Anal. Chem*., **73**, 1292 (2001).
11) E. P. Go, J. V. Apon, G. Luo, A. Saghatelian, R. H. Daniels, V. Sahi, R. Dubrow, B. F. Cravatt, A. Vertes, and G. Siuzdak, *Anal. Chem*., **77**, 1641 (2005).
12) G. Piret, H. Drobecq, Y. Coffinier, O. Melnyk, and R. Boukherroub, *Langmuir*, **26**, 1354 (2010).
13) N. H. Finkel, B. G. Pervo, O. D. Velev, and L. He, *Anal. Chem*., **77**, 1088 (2005).
14) Y. Xiao, S. T. Retterer, D. K. Thomas, J.-Y. Tao, and L. He, *J. Phys. Chem. C*, **113**, 3076 (2009).
15) Y. Chen and A. Vertes, *Anal. Chem*., **78**, 5835 (2006).
16) S. Alimpiew, S. Nikiforv, V. Karavanskii, T. Minton, and J. Sunner, *J. Chem. Phys*., **128**, 014711 (2008).
17) T. R. Northen, O. Yanes, M. T. Northen, D. Marrinucci, W. Uritboonthai, J. Apon, S. L. Golledge, A. Nordestrom, and G. Siuzdark, *Nature*, **449**, 1033 (2007).
18) C. T. Chen and Y. C. Chen, *Rapid Commun. Mass Spectrom*., **18**, 1956 (2004).
19) C. Y. Loa, J. Y. Lina, W. Y. Chena, C. T. Chena, and Y. C. Chen, *J. Am. Soc. Mass Spectrom*., **19**, 1014 (2008).
20) M. J. Kang, J. C. Pyun, Y. J. Choi, J. H. Park, J. G. Park, J. G. Lee, and H. J. Choi, *Rapid Commun. Mass Spectrom*., **19**, 3166 (2005).
21) M. Yuan, Z. Shan, B. Tian, B. Tu, P. Yang, and D. Zhao, *Microporous and Mesoporous Materials*, **78**, 37 (2005).
22) T. Seino, H. Sato, A. Yamamoto, A. Nemoto, M. Torimura, and H. Tao, *Anal. Chem*., **79**, 4827 (2007).
23) S. Okuno, R. Arakawa, K. Okamoto, Y. Matsui, S. Seki, T. Kozawa, S. Tagawa, and Y. Wada, *Anal. Chem*., **77**, 5364 (2005).
24) R. Nayak and D. R. Knapp, *Anal. Chem*., **79**, 4950 (2007).
25) V. Jokinen, S. Aura, L. Luosujärvi, L. Sainiemi, T. Kotiaho, S. Franssila, and M. Baumann, *J. Am. Soc. Mass Spectrom*., **20**, 1723 (2009).
26) H. Bi, L. Qiao, J. M. Busnel, V. Devaud, B. Liu, and H. H. Girault, *Anal. Chem*., **81**, 1177 (2009).
27) H. Yan, N. Xu, W. Y. Huang, H. M. Han, and S. J. Xiao, *Int. J. Mass. Spectrom*., **281**, 1 (2009).
28) L. C. Chen, J. Yonehama, T. Ueda, H. Hori, and K. Hiraoka, *J. Mass Spectrom*., **42**, 346 (2007).
29) (a) H. Kawasaki, T. Sugitani, T. Watanabe, T. Yonezawa, H. Moriwaki, and R. Arakawa, *Anal. Chem*., **80**, 7254 (2008). (b) A. Tarui, H. Kawasaki, T. Taiko, T. Watanabe, T. Yonezawa, and R. Arakawa, *J. Nanosci. Nanotechnol*., **9**, 159 (2009).
30) H. Kawasaki, T. Yao, T. Suganumaa, K. Okumura, Y. Iwaki, T. Yonezawa, T. Kikuchi, and R. Arakawa, *Chemistry–A European Journal,* **16**, 10832 (2010).
31) M. Najam-ul-Haq, M. Rainer, C. W. Huck, P. Hausberger, H. Kraushaar, and G. K. Bonn, *Anal. Chem*., **80**, 7467 (2008).
32) H. Kawasaki, N, Takahashi, H. Fujimori, K. Okumura, T. Watanabe, C. Matsumura, S. Takemine, T. Nakano, and R. Arakawa, *Rapid Commun. Mass Spectrom*., **23**, 3323 (2009).
33) T. Watanabe, K. Okumura, H. Kawasaki, and R. Arakawa, *J. Mass Spectrom*., **44**, 1443 (2009).
34) K. H. Lee, C. K. Chiang, Z. H. Lin, and H. T. Chang, *Rapid Commun. Mass Spectrom*., **21**, 2023 (2007).
35) C. T. Chen and Y. C. Chen, *Anal. Chem*., **77**, 5912 (2005).
36) T. L. Thompson and J. T. Yates, *Chem. Rev*., **106**, 4428 (2006).
37) J. M. Macak, H. Tsuchiya, A. Ghicov, K. Yasuda, R. Hahn, S. Bauer, and P. Schmuki, *Current Opinion in Solid State and Materials Science*, **11**, 3 (2007).
38) N. K. Kurumoto, R. A. Simão, and G. A. Soares, *Materials Characterization*, **58**, 114 (2007).
39) N. Martin, C. Rousselot, D. Rondot, F. Palmino, and R. Mercier, *Thin Solid Films*, **300**, 113 (1997).
40) H. W. Tang, K. M. Ng, W. Lu, and C. M. Che, *Anal. Chem*., **81**, 4720 (2009).
41) Y. Xiao, S. T. Retterer, D. K. Thomas, J. Y. Tao, and L. He, *J. Phys. Chem. C*, **113**, 3076 (2009).
42) G. Luo, Y. Chen, G. Siuzdark, and A. Vertes, *J. Phys. Chem. B*, **109**, 24450 (2005).
43) S. Dagan, Y. Hua, D. J. Boday, A. Somogyi, R. J. Wysocki, and V. H. Wyoski, *Int. J. Mass Spectrom*., **283**, 200 (2009).

44) G. Luo, Y. Chen, H. Daniels, R. Dubrow, and A. Vertes, *J. Phys. Chem. B*, **110**, 13381 (2006).
45) G. Luo, I. Marginean, and A. Vertes, *Anal. Chem*., **74**, 6185 (2002).
46) Y. Wada, T. Yanagishita, and H. Masuda, *Anal. Chem*., **79**, 9122 (2007).
47) L. P. Law, *Int. J. Mass Spectrom*., **290**, 72 (2010).
48) T. Watanabe, K. Okumura, K. Nozaki, H. Kawasaki, and R. Arakawa, *Rapid Commun. Mass Spectrom*., **23**, 3886 (2009).
49) L. Qiao, H. Bi, J.-M. Busnel, J. Waser, P. Yang, H. H. Girault, and B. Liu, *Chem. Eur. J*., **15**, 6711 (2009).
50) S. Alimpiew, S. Nikiforv, V. Karavanskii, T. Minton, and J. Sunner, *J. Chem. Phys*., **115**, 1891 (2001).
51) R. A. Kruse, X. Li, P. W. Bohn, and J. V. Sweedler, *Anal. Chem*., **73**, 3639 (2002).
52) Y. Chen, H. Chen, A. Aleksandrov, and T. M. Orlando, *J. Phys. Chem. C*, **112**, 6953 (2008).
53) S. A. Trauger, E. P. Go, Z. Shen, J. V. Apon, B. J. Compton, S. P. Bouvier, M. G. Finn, and G. Suizdak, *Anal. Chem*., **76**, 4484 (2004).
54) T. R. Northen, H. K. Woo, M. T. Northen, A. Nordström, W. Uritboonthail, K. L. Turner, and G. Suizdark, *J. Am. Soc. Mass Spectrom*., **18**, 1945 (2007).
55) Y. Nakaoka and Y. Nosaka, *Journal of Photochemistry and Photobiology A: Chemistry*, **110**, 299 (1997).

Keywords: Titania, SALDI-MS, Crystalline forms